

Mind the gap: Exact quantum dynamics in photonic crystals

Javier Prior,¹ Inés de Vega,² Alex W. Chin,^{2,3} Susana F. Huelga,² and Martin B. Plenio²

¹Departamento de Física Aplicada, Universidad Politécnica de Cartagena, Cartagena 30202, Spain

²Institut für Theoretische Physik, Albert-Einstein-Allee 11, Universität Ulm, D-89069 Ulm, Germany

³Theory of Condensed Matter Group, University of Cambridge,
J J Thomson Avenue, Cambridge, CB3 0HE, United Kingdom

(Dated: December 27, 2018)

Employing a recently developed numerically exact method for the description of arbitrary system-environment interactions, we analyze the full dynamics of an atomic system coupled to an environment with a gapped spectral density. This is a situation encountered for example for the radiation field in a photonic crystal and whose analysis has been so far been confined to limiting cases due to the lack of suitable numerical techniques. We show that both atomic population and coherences' dynamics can drastically deviate from the results predicted when using the rotating wave approximation, particularly in the strong coupling regime. Experimental conditions required to observe these corrections are also discussed.

Introduction. In the past decades, there has been an enormous interest in developing methods to control and modify the light field. In most cases, this has been achieved by building specific materials where the light matter interaction strongly modifies the characteristics of the free electromagnetic field. These new materials result in interesting technological applications as well as theoretical challenges. Important examples are microcavities [1], and metamaterials [2], which are designed respectively to strengthen the light-matter interaction, and to tailor the refraction index altering the flow of light in a non-trivial way [3, 4].

Within this scenario, photonic crystals (PC) provide one of the most interesting examples of artificially engineered materials. PCs [5–7] (see [8, 9] for basic reviews) are periodically microstructured compounds which tailor the vacuum electromagnetic density of states, creating specific frequency ranges, or gaps, where it vanishes. Reduction or suppression of the density of states within the band gap facilitates light localization and trapping in a bulk material [5, 6, 10], as well as the inhibition of spontaneous emission over a broad frequency range. Additionally, the density of states varies rapidly near the edge of the gap, whose frequency we will denote by ω_b , which implies that the correlation time of the vacuum fluctuations can be comparable to the characteristic time scales of atoms, quantum dots or NV centers embedded in the PC structure. Hence, an accurate description of the dynamics of systems in contact with highly structured environments, like the radiation field within PCs, may force us to go beyond the usual Markovian, and weak coupling approximations [11–13]. Therefore, a reliable method to describe the full system dynamics is highly desirable.

Here, we demonstrate that the efficient, numerically exact method developed in [14–16] (TEDOPA: Time Evolving Density with Orthogonal Polynomials Algorithm) is an excellent candidate to describe the dynamics of quantum systems, such as impurity atoms and quantum dots, within structured reservoirs. To this end, we

apply TEDOPA to describe the dynamics of a two level atom embedded in a photonic crystal. Our reason to chose such a system as a test bed is that, under certain limits and within the rotating wave approximation (RWA), it is known to be exactly solvable, thus providing an excellent arena to prove the reliability of our technique. Most importantly, the method deployed here is valuable in describing the exact dynamics beyond the simple RWA case. By evolving the system without invoking RWA, strong departures from the RWA result are found. We will show that when the system-environment coupling is strong, the atomic population dynamics differ from the RWA solution and an enhanced population trapping can be observed. When the system energy splitting, Δ , is much smaller than any other system and environment time scale, the RWA leads to an unphysical prediction for the system's coherence in the low frequency domain while TEDOPA allows to evaluate the exact dynamics across the whole frequency spectrum.

The model. We consider a single atom or quantum dot, modeled as a two-level system with transition frequency Δ , coupled to the modified radiation field that exists within a photonic crystal. The general interaction Hamiltonian can be written in interaction picture as follows ($\hbar = 1$)

$$H_{\text{int}} = \sum_{\lambda} g_{\lambda} \left(b_{\lambda}^{\dagger} \sigma^{-} e^{i\Delta_{\lambda}^{-} t} + b_{\lambda}^{\dagger} \sigma^{+} e^{i\Delta_{\lambda}^{+} t} + h.c. \right), \quad (1)$$

where σ^{\pm} are the atomic spin ladder operators, $\lambda \equiv \mathbf{k}, \xi, n$, with \mathbf{k} the field wave vector, $\xi = 1, 2$ the two polarization modes, and n denotes a band index [7, 8, 17]. In addition, the frequencies are defined as $\Delta_{\lambda}^{\pm} = \omega_k \pm \Delta$, and we consider $\omega_k = \omega_b + k^2/2m$, where m is an effective mass for the photon [7], corresponding to the dispersion relation of the radiation field for frequencies in the vicinity of a single band-gap edge (so that $n = 1$) with frequency ω_b . In the last relation, m is the effective mass acquired by a photon in a photonic crystal, as described in [7, 8]. The coupling constants in

Eq. (1) are $g_\lambda = \Omega \hat{e}_{\mathbf{k},n} \cdot \hat{u}_d / \omega_k$, with Ω a constant denoting the atom-field coupling strength, while $\hat{e}_{\mathbf{k},n}$ and \hat{u}_d denote the polarization and dipole moment unitary vectors respectively. The bosonic creation and annihilation operators of the photonic crystal light modes are b_k and b_k^\dagger , respectively for a mode of wavenumber k . The above Hamiltonian is not exactly solvable and the RWA is usually considered, so that the fast rotating terms (i.e. terms $\sim b_\lambda \sigma^-$ or $b_\lambda^\dagger \sigma^+$), are neglected with respect to the other (energy conserving) terms. In this case, $H_{\text{int}}^{\text{RWA}} = \sum_{\mathbf{k}} g_\lambda (b_k^\dagger \sigma^- e^{i\Delta_{\lambda}^- t} + h.c.)$. While the RWA is often a very good approximation, due to the existence of well separated time-scales, this is not always the case. In the case of strong coupling, we shall show that large deviations from RWA physics emerge, and that their description requires sophisticated numerical techniques.

Exact RWA solution – As noted above, when considering the RWA, the dynamics specified by the Hamiltonian Eq.(1) always remains in the one excitation sector and the time-dependent Schrödinger equation for the total atom-photonic crystal system wave function can be solved exactly [8, 18]. The probability amplitude $A(t)$ for an atom initially excited to remain in the excited state evolves in time as $\dot{A}(t) = - \int_0^t d\tau G(t-\tau) A(\tau)$, where $G(t) = \sum_{\mathbf{k}} \hat{g}_k^2 e^{-i\Delta_{\lambda}^- t} = \Omega^2 \frac{e^{i(\Delta t - \arctan[\omega_0 t])}}{(1+i\omega_0 t)^{3/2}}$, is the correlation function of the environment [18, 19]. A change of variable between k and $\omega(k)$, leads to expressing the correlation function as $G(t) = \frac{1}{\pi} \int_0^\infty d\omega J(\omega) e^{-i\omega t}$, with the spectral density given by

$$J(\omega) = \alpha \sqrt{\omega - \omega_b} e^{-\frac{\omega - \omega_b}{\omega_0}}, \quad (2)$$

where $\alpha = \frac{2\sqrt{2}\Omega^2}{8\pi^3\sqrt{\pi}\omega_0^{3/2}} \left(\frac{l}{X_0}\right)^3$, where l is the linear dimension of the unit PC cell, and we have considered a renormalized coupling constant $\hat{g}_k = g_k e^{-k^2 X_0^2/2}$. The factor $e^{-k^2 X_0^2/2}$ physically comes from the fact that when calculating the coupling, one should take into account that the electronic wave function [20] has a finite width X_0 . This represents the finite region in which the electron moves around the nucleus. This factor (often neglected within the dipolar approximation), leads to the momentum cut-off $k_0 = 2\pi/X_0$, the frequency cut-off $\omega_0 = \omega_{k_0}$ and the suppression of a singularity at the origin of times in the correlation function (such singularity appears for instance in [21]). Using the Laplace transform method, a numerical solution for $A(t)$ can always be obtained. In contrast, an analytical solution requires additional approximations, namely that the system frequencies are very small compared to the cut frequency ω_0 , so that $\omega_0 \gg \Omega, \Delta$, and that all relevant time scales obey $t \ll 1/\omega_0$ [7, 22]. Under these conditions, several dynamical regimes exist depending on the value of the parameter $\hat{\Delta}_L = \Delta_L + \omega_s$, where $\Delta_L = \Delta - \omega_b$ and ω_s is a frequency that depends on the coupling strength [18, 19]. In this regard, for $\hat{\Delta}_L > 0$ the atom is not

excited in the stationary state (i.e. relaxes completely to the ground state), whereas for negative values of $\hat{\Delta}_L$ there is a stationary residual excited atomic population (corresponding to a situation where the emitted photon remains localized nearby the atom). Thus, tuning $\hat{\Delta}_L$ from negative to positive values leads to a cross-over between two distinct regimes.

Beyond the RWA – When the RWA is not applicable, the dynamics of the global atom-light system cannot be described in the one-excitation manifold, and the direct wave function approach presented above becomes intractable. However, a new technique has recently emerged in the theory of open quantum systems which allow this task to be performed with numerical exactitude. This technique [14, 15] employs time-adaptive density matrix re-normalisation group algorithm to compute the evolution of the full atom and light field wavefunction. The first step of this method transforms the atom-light Hamiltonian into a suitable 1D form [14, 15, 23]. Starting from the Hamiltonian of Eq. (1) in the Schrödinger picture, $H = \frac{1}{2}\Delta(1 + \sigma_z) + \sum_k g_k \sigma_x (b_k + b_k^\dagger) + \sum_k \omega_k b_k^\dagger b_k$, it has been shown in [14, 15] that a unitary transformation on the bosonic degrees of freedom can always bring this Hamiltonian into the form $\tilde{H} = \frac{1}{2}\Delta(1 + \sigma_z) + \sqrt{\eta} \sigma_x (a_0 + a_0^\dagger) + \sum_{n=0}^{\infty} (\epsilon_n a_n^\dagger a_n + t_n a_n^\dagger a_{n+1} + t_n a_{n+1}^\dagger a_n)$, if the spectral function of the bosonic modes are specified [15]. The bosonic operators a_k, a_k^\dagger are the creation and annihilation operators of the modes in the transformed picture. All dynamical information about the original atom-photon interactions are encoded faithfully in the local frequencies ϵ_n , intra-chain t_n and system-environment $\eta_0 = \int_0^\infty J(\omega) d\omega$ couplings of the chain representation of the light field. These parameters can be expressed analytically using orthogonal polynomials, and computed numerically for arbitrary spectral functions (TEDOPA), as discussed in [14, 15, 24]. After this procedure it now becomes possible to apply time-adaptive density matrix renormalisation methods [25, 26] to simulate the unitary evolution of the total atom and chain wavefunction $|\Psi(t)\rangle$. From $|\Psi(t)\rangle$, the real-time expectation of any observable O_a of the atom can be simply calculated by evaluating $\langle O_a(t) \rangle = \langle \Psi(t) | O_a | \Psi(t) \rangle$.

Exact Numerical Results – The cross-over occurring when tuning $\hat{\Delta}_L$ from negative to positive values can also be observed when considering the exact numerical solution of $\dot{A}(t)$, but until now it had only been described within the RWA. Thus, a question that remained open is whether this transition is a consequence of the RWA, or can also be observed in situations where the RWA is invalid. Fig. 1 shows the stationary atomic population for an initially excited atom, with respect to the atomic frequency Δ . In this Figure, the mentioned cross-over from a photon-atom bound state to a total relaxed state is sharper within the RWA than when the full Hamiltonian Eq. (1) is simulated. We note also that the cross-over

indeed occurs at a slightly shifted frequency relative to RWA and that in neither case does the cross-over occur exactly at $\Delta = \omega_b$. Also, the cross-over occurs at larger Δ for the full Hamiltonian because the high-energy (fast) modes of the light field renormalise (suppress) the effective energy of the atomic transition so that such effective energy actually lies below the band gap. As we shall see, these renormalisation effects are very different in the RWA and the non-RWA models, resulting in the different shifts and cross-over curves. A sharp transition at $\Delta_L = 0$ only appears as $\omega_0 \rightarrow \infty$ [8, 18], and when the coupling is very weak. However one should also note that the cross-over width in Fig. (1) is over emphasised by the logarithmic scale.

Figure 1 also shows that the residual population in the excited state remains larger in the simulations of the full Hamiltonian relative to results obtained within the RWA approximation. This arises due to *multi-photon* effects which cannot be described in RWA. For $\Delta \gg \omega_b$, the atom is able to exchange energy with the light field via photon emission/absorption, and at long times relax towards the ground state of the atom-photon Hamiltonian. However, the interactions with the bath alter the effective eigenstates of the system, leading to the residual excited state populations in the atom-light field ground state. This state can be approximately described by the variational polaron ground state first suggested in [27]. Following the procedure set out in [27], the reduced density matrix of the atom's variational polaron ground state - in the basis $|\pm\rangle$, where $|\pm\rangle$ are the eigenstates of σ_x - is given by $\rho_{gs}^{atom} = \frac{1}{2}|+\rangle\langle+| + \frac{1}{2}|-\rangle\langle-| - \Phi|-\rangle\langle+| - \Phi|+\rangle\langle-|$ where $\Phi = \tilde{\Delta}/\Delta$ and $\tilde{\Delta}$ is determined from the implicit equation

$$\tilde{\Delta} = \Delta \exp \left[-\frac{2}{\pi} \int_{\omega_b}^{\infty} \frac{d\omega J(\omega)}{(\omega + \tilde{\Delta})^2} \right]. \quad (3)$$

The off-diagonal elements of the density matrix are suppressed by dressing, or polaronic, correlations (state-dependent coherent displacements) between the bath and atomic states $|\pm\rangle$. These correlations effectively suppress the effective energy gap ($\tilde{\Delta} \rightarrow 0$) between the atomic states $|\uparrow\rangle$ and $|\downarrow\rangle$, through the reduced overlap of the displaced light mode wave functions which dress the states $|\pm\rangle$ [16, 27]. From the density matrix ρ_{gs}^{atom} , the population in the excited atomic level is $P_{\uparrow} = \frac{1}{2}(1 - \Phi)$. For large $\alpha, \omega_b \ll \Delta \ll \omega_0$ the approximate self-consistent solution of Eq. (3) is $\tilde{\Delta} \approx \Delta \left(1 - \frac{\alpha}{\sqrt{\Delta}}\right)$. This shows that as Δ gets larger, the re-normalisation from the environment gets smaller, so $\Phi \rightarrow 1$ and $P_{\uparrow} \rightarrow 0$. For the parameters in Fig. (1), we find that the solution of Eq. (3) with $\Delta = 30$ gives $P_{\uparrow} = 0.026$ which agrees with the data very well. Note that these formulas are only valid when the atom is able to relax to the polaronic ground state, which occurs for $\Delta > \omega_b$ [28]; at $\Delta < \omega_b$, relaxation is blocked by energy conservation. In this case

a better prediction for the residual population is to assume that the final state is the dressed excited state, in which case the final population is $P_{\uparrow} = \frac{1}{2}(1 - \Phi)$, with Φ obtained from Eq. (3). In the RWA approximation the analytical theory predicts a total de-excitation of the atom at large $\Delta > \omega_b$. This is seen in Fig. (1), although the transition is slightly smoothed out by the finite value of ω_0 used in the simulations, as discussed above.

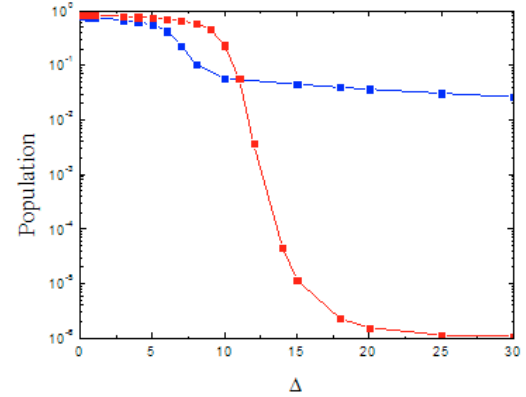


FIG. 1: Stationary state atomic population in logarithmic scale, using the RWA (red squares) and the complete Hamiltonian (blue squares), represented with respect to Δ . The initial state is a fully excited system, and we have used $\alpha = 1$, $\omega_0 = 100$, $\omega_b = 5$, and $\omega_c = 800$.

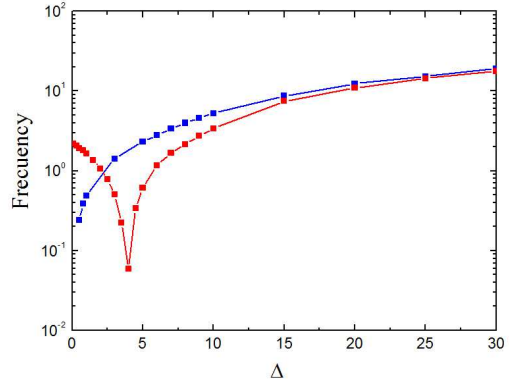


FIG. 2: Frequency of coherence oscillations in a logarithmic scale, using the RWA (red squares) and the complete Hamiltonian (blue squares) as a function of Δ for an initially-prepared superposition of ground and excited states. Parameters are $\alpha = 1$, $\omega_0 = 100$, $\omega_b = 5$, and $\omega_c = 800$.

Let us consider now the evolution of the system coherences $\langle \sigma_x(t) \rangle$, starting from an initial condition where $\langle \sigma_x(0) \rangle = 1$. In the absence of the radiation field, we would expect that $\langle \sigma_x(t) \rangle = \cos(\Delta t)$ and in its presence these coherent oscillations would - in a simple markovian picture - become damped and shifted to lower frequencies [11, 29]. Figure (2) shows the frequency of the coherence oscillations for the full Hamiltonian and

the RWA for different values of the atomic frequency Δ . Within the RWA, the behaviour can be understood by looking at the pole structure of the exact solution expressed as a Laplace transform. For our initial condition, the Laplace transform of $\langle \sigma_x(t) \rangle$ can be expressed as $\mathcal{L}[\langle \sigma_x(t) \rangle] = \frac{1}{2}(s + i\Delta + \mathcal{L}[G(t)])^{-1} + h.c..$ Although the Laplace transform $\mathcal{L}[G(t)]$ can be computed exactly, we can qualitatively understand the key features of Fig. (2) by considering just an expansion to lowest order in the small quantities $\Delta/\omega_0, \omega_b/\omega_c$. This gives $\mathcal{L}[G(t)] = -i\alpha\sqrt{\frac{\omega_0}{\pi}} + \alpha\sqrt{is - \omega_b}$, with α given in Eq. (2). When $\Delta \rightarrow 0$, the poles of $\mathcal{L}[\langle \sigma_x(t) \rangle]$, s_{\pm} , are approximately $s_{\pm} \approx \pm i\alpha(\sqrt{\frac{\omega_0}{\pi}} - \alpha\sqrt{\omega_b})$. This leads to the convergence of the oscillation frequency to a finite value when $\Delta \rightarrow 0$ as it is observed in Fig. (2) for the RWA. The poles are completely imaginary, and these oscillations are undamped, although there is a slight loss of amplitude due to dynamical transients. For larger Δ , the poles now appear at approximately $s_{\pm} \approx \pm i(\Delta - \alpha\sqrt{\frac{\omega_0}{\pi}} + \alpha\sqrt{\Delta - \omega_b})$, leading to a reduction of the effective oscillation frequency as the Δ term compensates the frequency shift coming from the environment. At even higher values of Δ , the poles are dominated by the contribution from Δ and are approximately $s_{\pm} \approx \pm i\Delta + \alpha\sqrt{\Delta}$. The oscillation frequency is now proportional to Δ and has acquired a real part which damps the oscillations with a rate given by the Fermi Golden Rule as $\Gamma = J(\Delta)$. This is the result one would obtain by a standard weak coupling and Markovian approximation to the open-system dynamics with the spectral density of Eq. (2).

The behaviour of the oscillation frequency for small Δ is clearly a pathology of the RWA approximation and arises because of a poor treatment of the low frequency modes in the problem. The breakdown of the RWA manifests itself in the renormalisation of the atomic energy Δ which leads to a shift in Δ that is larger than Δ itself, an effect which produces the minimum in Fig. (2) and the convergence to a finite oscillation frequency as $\Delta \rightarrow 0$. The correct behaviour in this limit can be calculated exactly for the full Hamiltonian (1), as for $\Delta = 0$ the model corresponds to the exactly solvable independent boson model [30]. This predicts that $\langle \sigma_x(t) \rangle$ does not oscillate and remains constant. This limiting behaviour is correctly described by the TEDOPA simulation of the full Hamiltonian. For small, but finite Δ , the frequency simply increases monotonically with Δ and TEDOPA results agree very well with the prediction $\tilde{\Delta} \approx \Delta \exp(-\alpha/\sqrt{\omega_b}) + O(\frac{\omega_b}{\omega_0})$ given by adiabatic renormalisation theory (a simplified version of Silbey-Harris theory which is valid in the small Δ limit) [29].

Considering a photonic crystal with a gap in the optical region, couplings of the order of $\alpha^2 = 10^5 - 10^6 \text{ Hz}$ may be achieved, which in our units [31] would be $\alpha^2 = 10^{-9} - 10^{-10}$. In order to enlarge the coupling, and thus reach the regime discussed in this paper, there are different possibilities. One may consider for instance

photonic crystals with narrow band-widths $\Delta\omega$, what would give rise to smaller cut-off frequencies $\omega_0 = \omega_{k_0} = \omega_b + l\Delta\omega k_0^2/3$. Here we have considered the fact that the $\hbar/2m = l^2\Delta\omega/3$ [17]. Strong system-environment coupling can also be achieved when strong collective effects produce an enhanced effective system-environment coupling [32, 33]. The simplest situation in which this enhancement can be achieved is by considering a collection of N atoms uniformly interacting with the radiation field or environment, or similarly, when describing the collective coupling of a spin system to superconducting resonators [34]. In this case, for a single excitation in the system (i.e. only one atom in the ensemble is excited), the situation is completely analogous to the one described here, except for the fact that the coupling is enhanced by a factor N^2 in the photonic crystal case [7]. Thus, a value $\alpha_{\text{eff}}^2 = N^2\alpha^2 = 1$ would be achieved if we have a high enough number of impurity atoms. Of particular interest is also the multi-excitation regime for this configuration. A spontaneous polarization phenomenon, in which the atomic coherences grows from zero to a finite value, is predicted to occur for atoms in photonic crystal-like environments, when the atomic frequencies are resonant with the band edge $\Delta = \omega_b$ and when considering the semi-classical and RW approximations [7, 18, 19]. The results in our work show strong differences in the behaviour of single atom coherences with and without considering the RWA, particularly for small Δ_L , and suggest that applying the novel technique [14, 15] for treating the system-environment interaction in the analysis of multi-atomic systems will shed new light into this and other intriguing collective phenomena. Other possible enhancement factors for the coupling coefficient would involve placing the atom within a photonic crystal cavity [35]. In a more general scenario, one may consider a situation where the effective system-environment interaction, characterised by $\sqrt{\eta_0}$ in our chain representation of the system, is larger than the typical frequencies of the light field, ω_b . As we have shown, in this regime the ground and excited atomic states are entangled with the light field through polaronic correlations, and these are very similar to the shifted vacuum states which appear in the recent theory of *ultrastrong coupling* in quantum wells and circuit QED where this regime can be realised [36, 37]. In conclusion, this work has demonstrated that our TEDOPA method for the treatment of system environment interaction has allowed to reveal strong deviations between the exact and approximate solutions in physical models of practical importance and hence suggest its use in a wide variety of settings where non-perturbative system environment interactions are expected to play a role.

We thank A. Imamoglu for his comments at the start of this project, the EU-STREPs HIP and PICC and the EU Integrated project QESSENCE, as well as the Alexander von Humboldt foundation for support. J.P. was supported by the Fundación Séneca Project No.

11920/PI/09-j and the Ministerio de Ciencia e Innovación Project No. FIS2009-13483-C02-02, I.d.V was partially supported by the Ministerio de Ciencia e Innovación Project No. FIS2010-19998, AWC acknowledges the support of the Winton Programme for the Physics of Sustainability.

[1] K. Vahala, *Nature* **424**, 839 (2003).

[2] J.B. Pendry, A.J. Holden, D.J. Robbins, and W.J. Stewart, *IEEE Trans. Microwave Theory Tech* **47**, 20752084 (1999).

[3] J. B. Pendry, D. Schurig, and D. R. Smith, *Science* **312**, 1780 (2006).

[4] K. L. Tsakmakidis, A.D. Boardman and O. Hess, *Nature Photonics* **450**, 397 (2007).

[5] E. Yablonovitch, *Phys. Rev. Lett.* **58**, 2059 (1987).

[6] S. John, *Phys. Rev. Lett.* **58**, 2486 (1987).

[7] S. John and T. Quang, *Phys. Rev. Lett.* **74**, 3419 (1995).

[8] M. Woldeyohannes and S. John, *J. Opt. B: Quantum Semiclass. Opt.* **5**, R43 (2003).

[9] D. Angelakis, E. Paspalakis, and P. Knight., *Contemporary Phys.* **45**, 303 (2004).

[10] T. Baba, *Nature Photonics* **2**, 465 (2008).

[11] H. Breuer and F. Petruccione, *The theory of Quantum Open Systems* (Oxford Univ. Press, 2002).

[12] A. Rivas, A. Plato, S. Huelga, and M. Plenio, *New. J. Phys.* **12**, 113032 (2010).

[13] A. Rivas and S. F. Huelga, *Open Quantum Systems. An Introduction* (Springer, Heidelberg) (2011).

[14] J. Prior, A. W. Chin, S. F. Huelga, and M. B. Plenio, *Phys. Rev. Lett.* **105**, 050404 (2010).

[15] A. W. Chin, A. Rivas, S.F. Huelga and M.B. Plenio, *J. Math. Phys* **51**, 092109 (2010).

[16] A. W. Chin, J. Prior, S. F. Huelga, and M. B. Plenio, *Phys. Rev. Lett.* **107**, 160601 (2011).

[17] I. de Vega, D. Alonso, and P. Gaspard, *Phys. Rev. A* **71**, 023812 (2005).

[18] I. de Vega, D. Porras, and I. Cirac, *Phys. Rev. Lett.* **101**, 260404 (2008).

[19] C. Navarrete-Benlloch, I. de Vega, D. Porras, and J. I. Cirac, *New J. Phys.* **13**, 023024 (2011).

[20] D.F. Walls and G.J. Milburn, *Quantum Optics* (Springer Verlag, 2008).

[21] M. Florescu and S. John, *Phys. Rev. A* **69**, 053810 (2004).

[22] S. John and T. Quang, *Phys. Rev. A* **50**, 1764 (1994).

[23] R. Bulla, H.-J. Lee, N.-H. Tong, and M. Vojta, *Phys. Rev. B* **71**, 045122 (2005).

[24] A. W. Chin, S. F. Huelga, and M. B. Plenio, in *Semiconductors and Semimetals* **85**, 115 - 144, edited by U. Würfel, M. Thorwart, E.R. Weber and C. Jagadish, (Academic Press, 2011).

[25] G. Vidal, *Phys. Rev. Lett.* **91**, 147902 (2003).

[26] U. Schollwöck, *Ann. Phys. N.Y.* **326**, 96 (2001).

[27] R. Silbey and R. A. Harris, *J. Chem. Phys.* **80**, 2615 (1984).

[28] In these inequalities, the shift ω_s has been neglected. .

[29] A. J. Leggett *et al.*, *Rev. Mod. Phys* **59**, 1 (1987).

[30] G. D. Mahan, *Many-Particle Physics* (Plenum Press, New York, 1981).

[31] Since both the atomic resonant frequency and PC gap are in the optical region, our frequency units are $1\omega_u = 10^{15} \text{ Hz}$.

[32] R. Dicke, *Physical Review*, **vol. 93**, 99 (1954).,

[33] A.V. Andreev, V.I. Emel'yanov and Yu. A. Il'inskii, *Cooperative effects in optics, superradiance and phase transitions* (Malvern Physics series, 1993).

[34] Y. Kubo, F. R. Ong, P. Bertet, D. Vion, V. Jacques, D. Zheng, A. Drau, J.-F. Roch, A. Auffeves, F. Jelezko, J. Wrachtrup, M. F. Barthe, P. Bergonzo, and D. Esteve, *Phys. Rev. Lett.* **105**, 140502 (2010).

[35] J. D. Joannopoulos, *Photonic crystals: molding the flow of light* (Princeton University, 2008).

[36] C. Nataf and P. Ciuti, *Phys. Rev. Lett.* **104**, 023601 (2010).

[37] C. Nataf and P. Ciuti, *Phys. Rev. Lett.* **107**, 190402 (2011) .